Combined Talk

Part one:

TH/3-1Ra

Toward An Emerging Understanding of ELM Crashes and Energy Loss Scaling

X.Q.Xu[1], P.W.Xi[1,2], P.H.Diamond[3,4], J.F.Ma[1,5], C.H.Ma[1,2], A.Dimits[1], I.Joseph[1], M.V.Umansky[1], B. Gui[1,6], G.Q.Li[1,6], T.Y.Xia[1,6], B.Dudson[7], P.B.Snyder[8]

Part two:

TH/3-1Rb

Advanced Divertor Analysis of HL-2M

G.Y. Zheng[1], X.Q. Xu[2], D.D. Ryutov[2], T.Y. Xia[3] and Y.D. Pan[1], Z.H. Wang[1]

SWIP Southwestern Institute of Physics

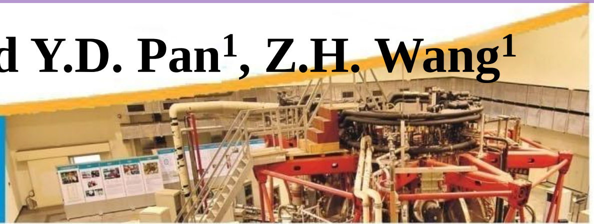

Toward An Emerging Understanding of ELM Crashes and Energy Loss Scaling

BOUT++
Boundary Plasma Turbulence Code

X.Q.Xu[1], P.W.Xi[1,2], P.H.Diamond[3,4], J.F.Ma[1,5], C.H.Ma[1,2], A.Dimits[1], I.Joseph[1], M.V.Umansky[1], B. Gui[1,6], G.Q.Li[1,6], T.Y.Xia[1,6], B.Dudson[7], P.B.Snyder[8]

[1]Lawrence Livermore National Laboratory, Livermore, California 94550, USA
[2]School of Physics, Peking University, Beijing, China
[3]WCI Center for Fusion Theory, National Fusion Research Institute, Daejon, R. Korea
[4]Center for Astrophysics and Space Sciences and Dept. of Phys., UC San Diego, La Jolla, CA 92093, USA
[5]Institute for Fusion Studies, University of Texas, Austin, TX, 78712, USA
[6]Institute of Plasma Physics, Chinese Academy of Sciences, Hefei 230031, China
[7]University of York, Heslington, York YO10 5DD, United Kingdom
[8]General Atomics, San Diego, California 92186, USA

Presented at
the 25th IAEA Fusion Energy Conference (FEC 2014),
St Petersburg, Russian Federation
13 - 18 October 2014

This work was performed under the auspices of the U.S. DoE by LLNL under Contract DE-AC52-07NA27344 , LLNL LDRD project 12-ERD-022 and is supported by the China NSF under Contract No.10721505, the National Magnetic Confinement Fusion Science Program of China under Contracts No. 2011GB107001. LLNL-PRES-661094.

Principal Results

As the pedestal collisionality decreases,
Two factors determine if a single mode amplitude can grow to a large magnitude to trigger an ELM

- **Linear growth rate**
- **Nonlinear growth time**

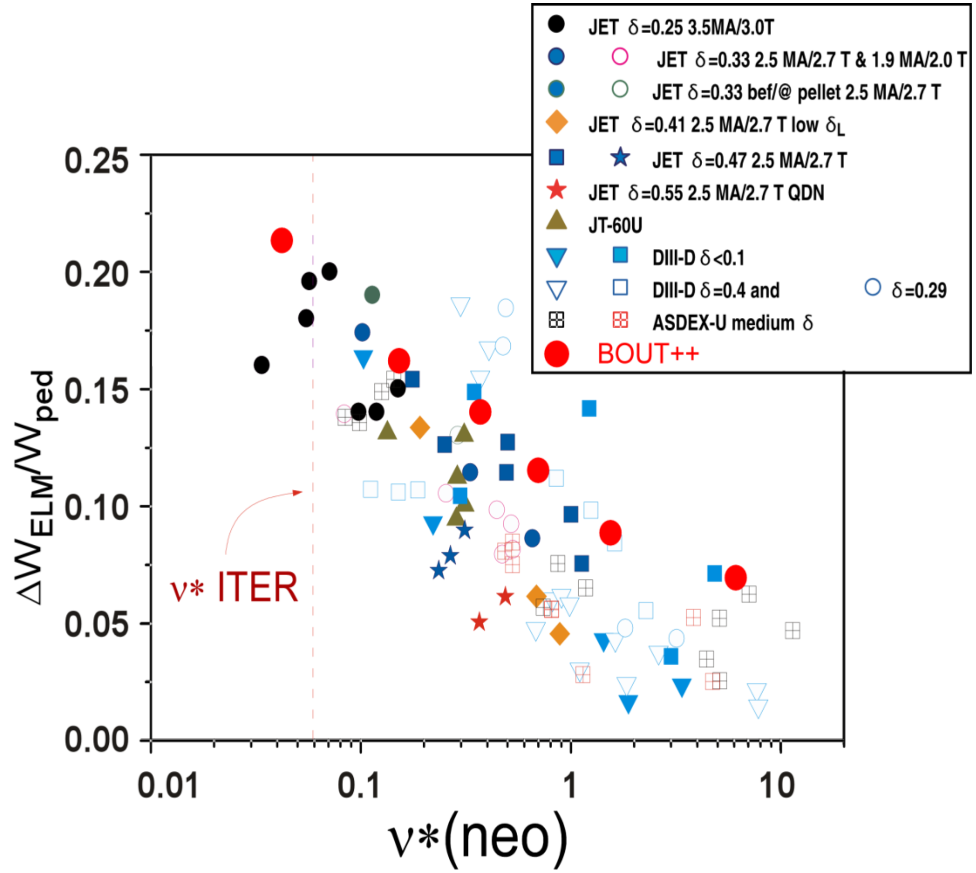

Linear results

The width of the growth rate spectrum γ(n) becomes narrower and the peak growth shifts to lower n

Nonlinear results

The growth time of linear drive is determined by nonlinear process via phase evolution for large ELM crash

Narrow mode spectrum → Weak nonlinear Phase Scattering →Long PCT →Large ELMs

BOUT++ simulations show consistent collisionality scaling of ELM energy losses with ITPA multi-tokamak database

As the edge density (collisionality) increases, the growth rate of the P-B mode increases for high n but decreases for low n (1<n<5)

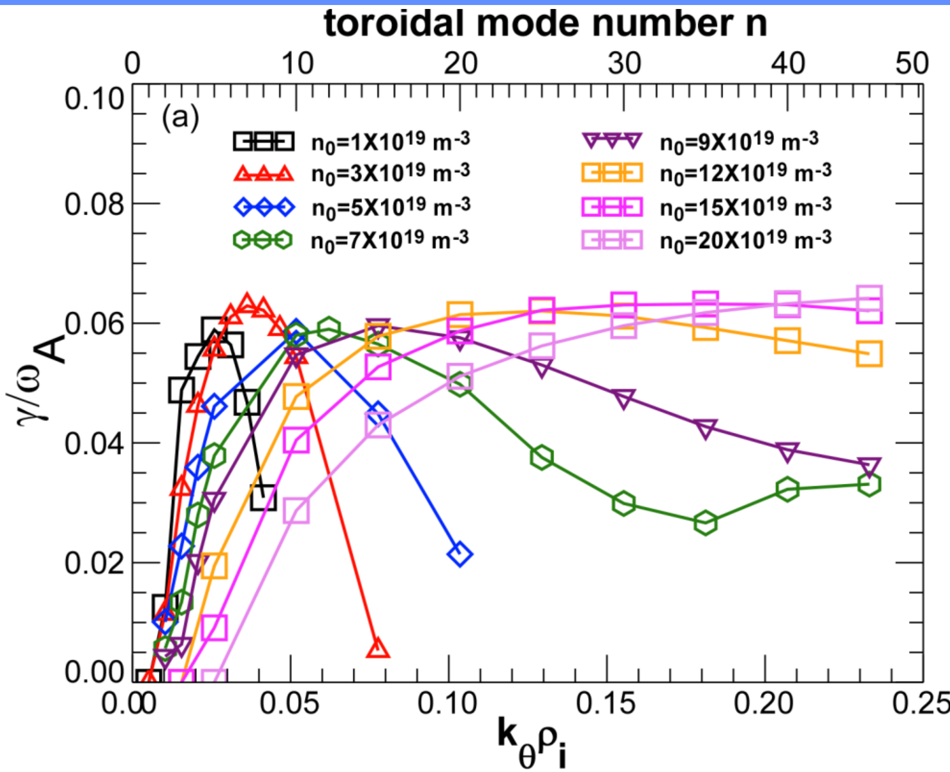

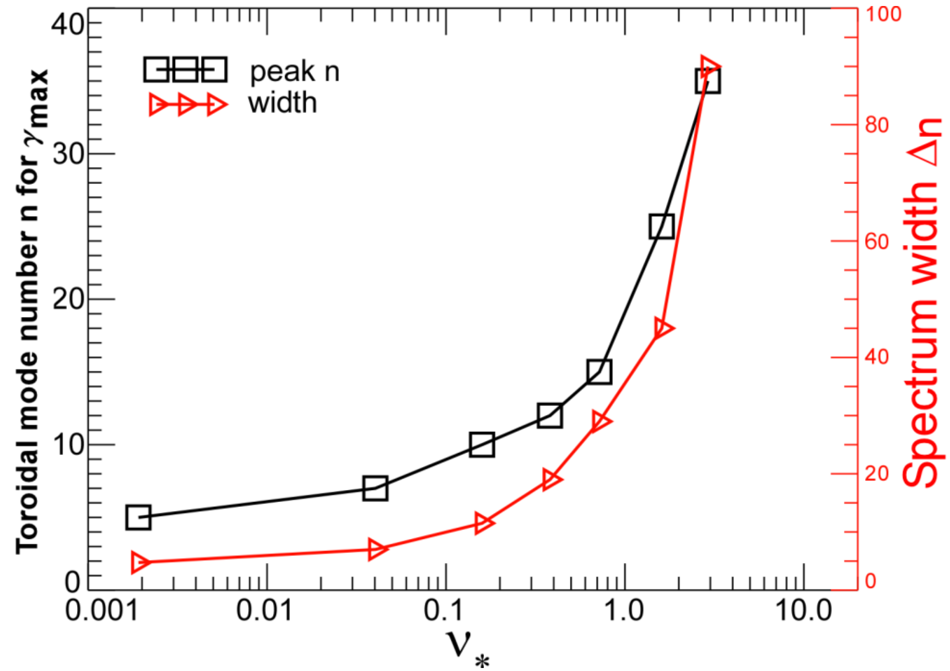

- ❑ **The ballooning term dominates the high n modes. Because ion diamagnetic drift is inversely proportional to the density for fixed pressure, when density increases, the ion diamagnetic stabilization decreases and growth rate increases.**

- ❑ **The kink term dominates the low n modes. Therefore, as the density increases, the edge current decreases and growth rate decreases.**

The growth time of linear drive is determined by nonlinear process via phase evolution for large ELM crash

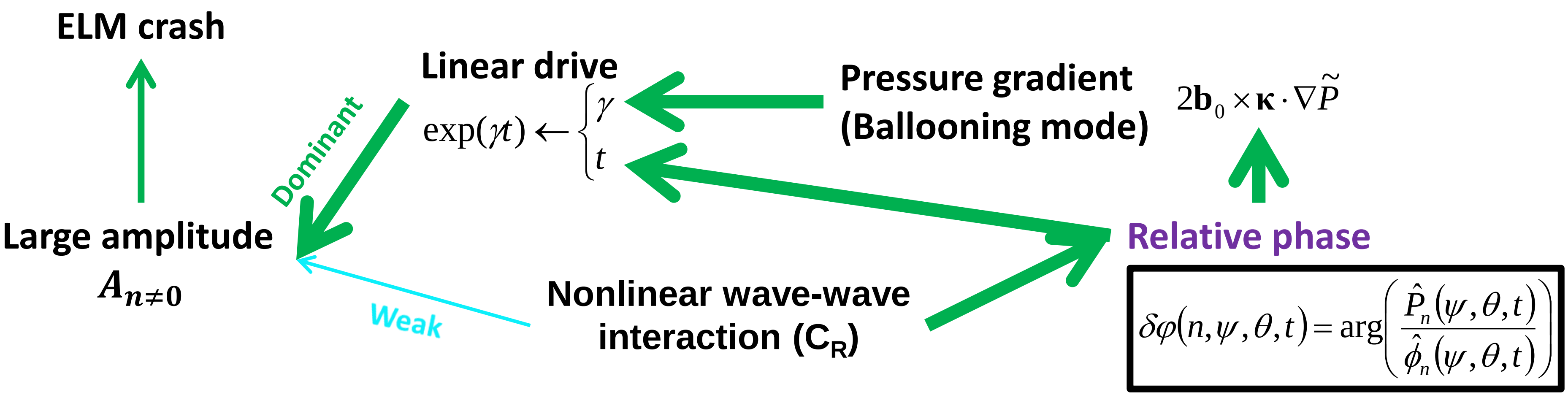

ELM size vs nonlinearity C_R

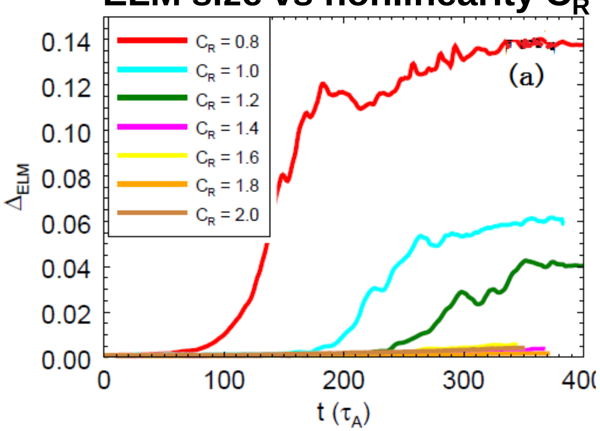

PCT vs nonlinearity C_R

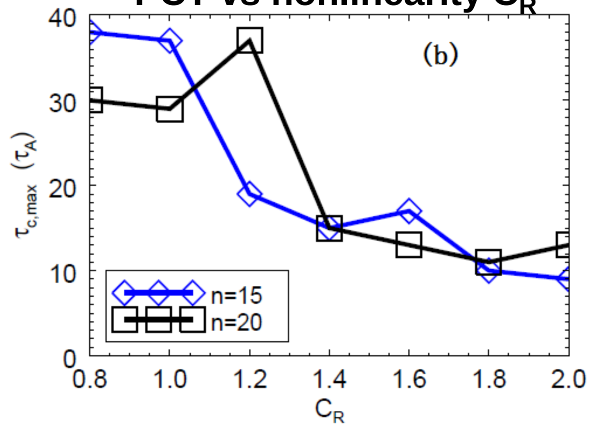

$$\frac{\partial \varpi}{\partial t} + C_R \frac{\mathbf{b}\times\nabla\phi}{B}\cdot\nabla\varpi = RHS$$

Phase coherence time (PCT, τ_c): the length of time duration of the **relative phase** for linear growth

→Linear theory/simulations: unchanged $\delta\varphi \Rightarrow \tau_c \to \infty$

→The growth time is determined by nonlinear Phase Scattering

Xi, Xu, Diamond, Phys. Plasmas 21, 056110 (2014)

BOUT++ simulations show consistent collisionality scaling of ELM energy losses with ITPA multi-tokamak database

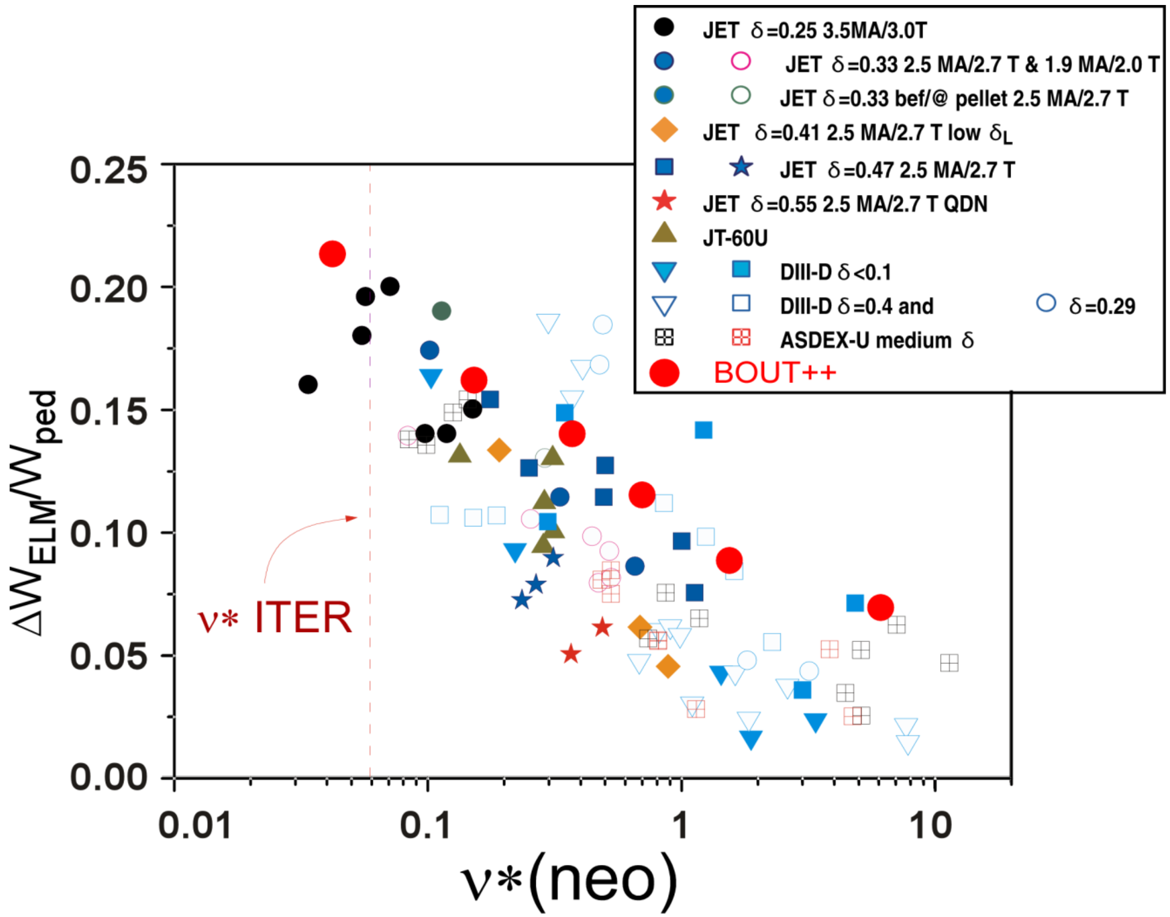

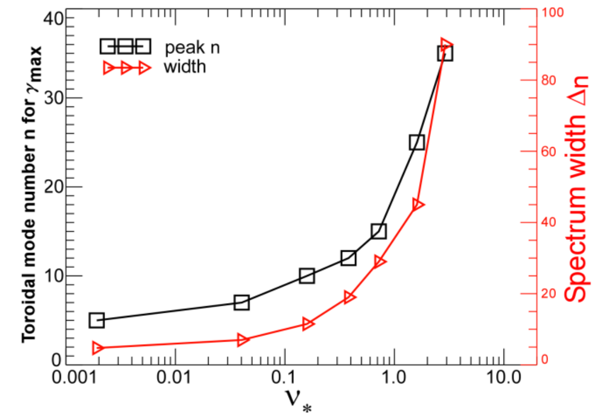

Two factors determine if a single mode amplitude can grow to a large magnitude to trigger an ELM

- **Linear growth rate**
- **Nonlinear growth time**

$$\exp(\gamma\, t) \leftarrow \begin{cases} \gamma <- \text{linear} \\ t <- \text{nonlinear} \end{cases}$$

As the edge collisionality decreases, both linear and nonlinear physics set ELM energy loss

- **Linearly, the dominant P-B mode shifts to lower n and the spectrum width of the linear growth rate decreases**
- **Nonlinearly,**
  Narrow mode spectrum → Weak nonlinear Phase Scattering →Long PCT →Large ELMs

BOUT++ simulations show the small change in ELM affected volume with increasing plasma density, consistent with experiments

Profile of surface-averaged pressure perturbation

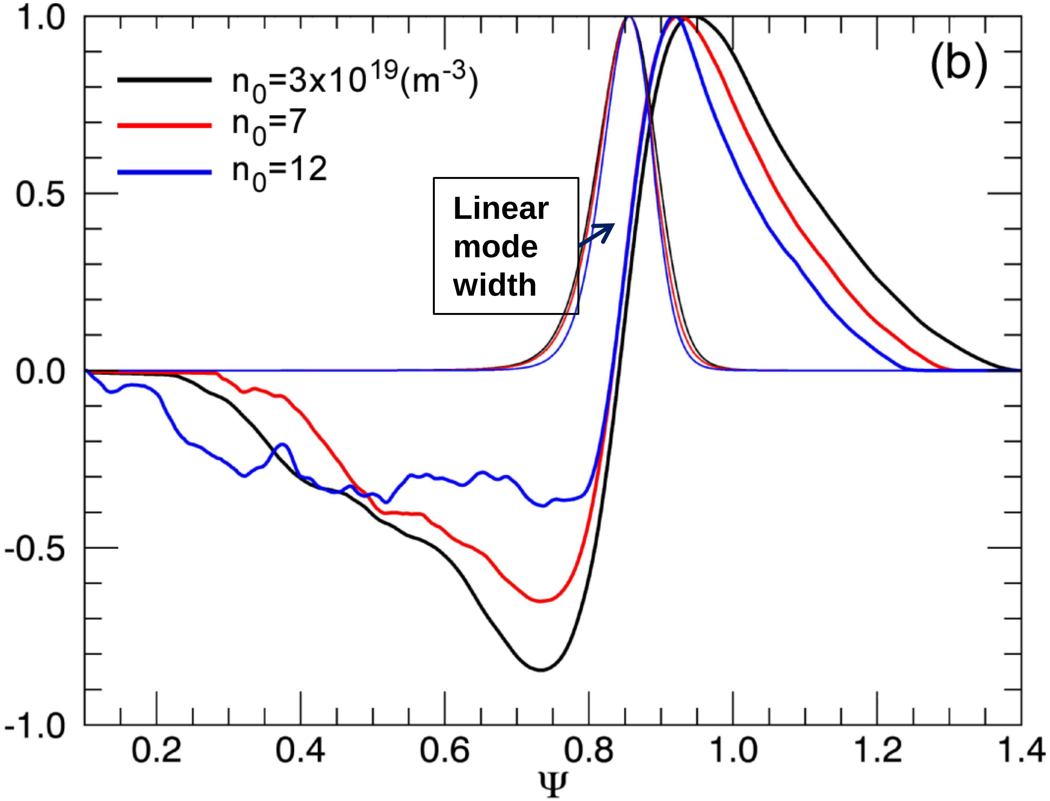

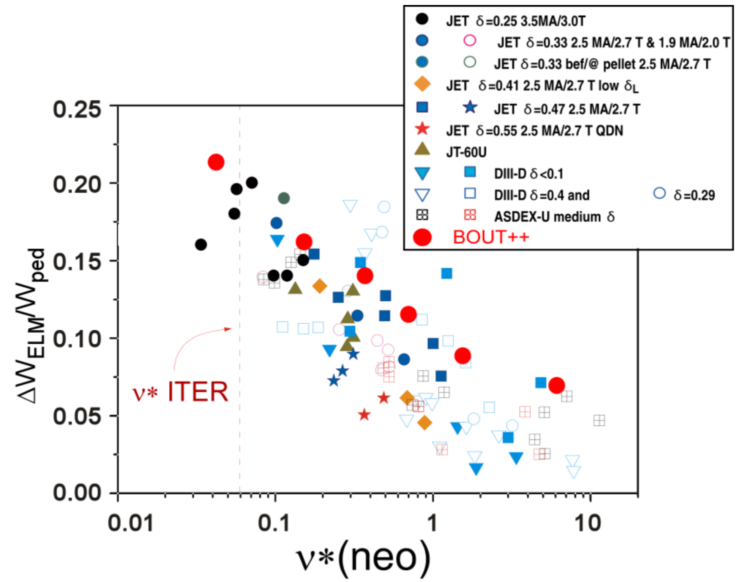

- ❑ **The reduction of ELM energy loss with increasing density (or collisionality) is accompanied by a decrease of the perturbation to the pressure caused by the ELM in an approximately constant volume**
- ❑ **As the edge collisionality decreases, the dominant P-B mode shifts to lower n and the spectrum width decreases**

Narrow mode spectrum → Weak nonlinear Phase Scattering →Long PCT →Large perturbation

Linear criterion for the onset of ELMs $\gamma > 0$ is replaced by the new nonlinear criterion $\gamma > \gamma_c$

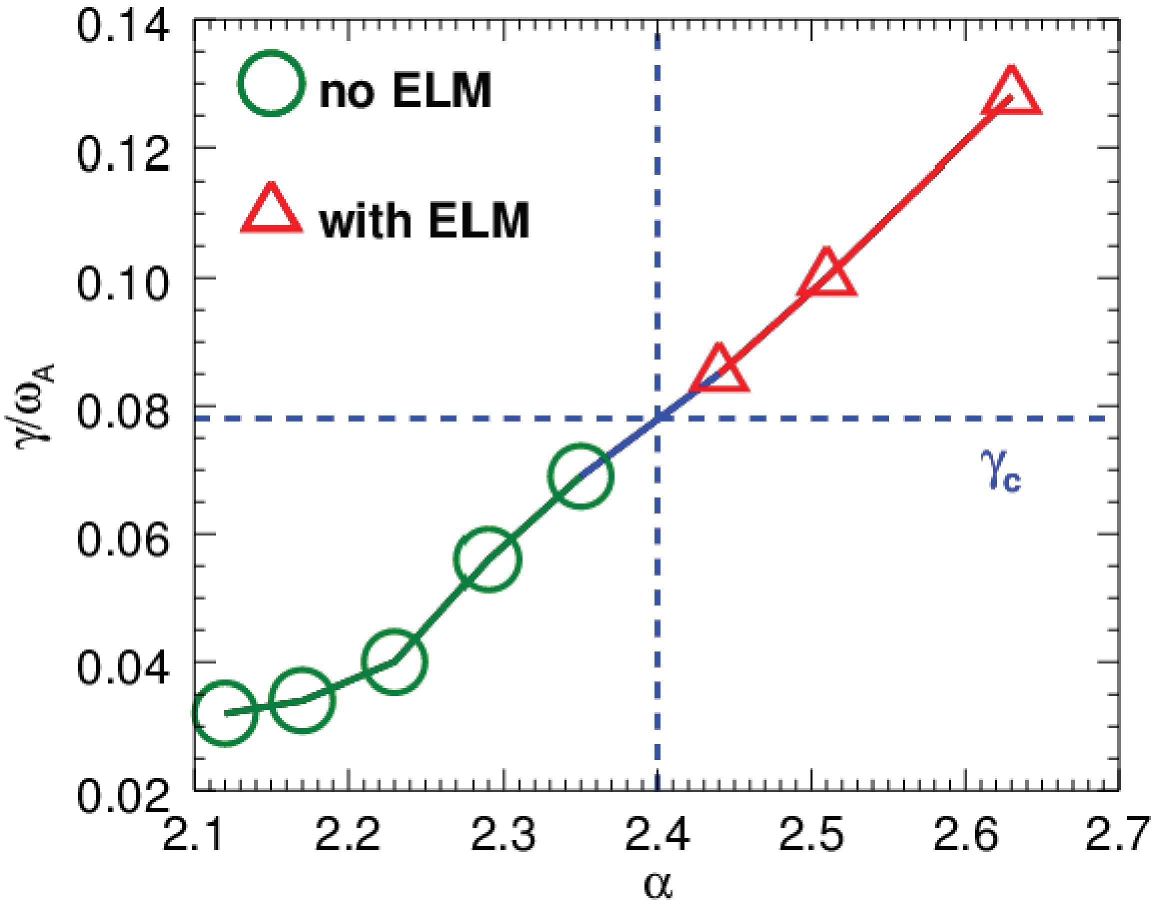

- **Criterion for the onset of ELMs**

$$\gamma\tau_c > \ln 10 \Rightarrow \gamma > \frac{\ln 10}{\tau_c} \equiv \gamma_c$$

- **Linear limit**

$$\lim_{\tau_c \to \infty} \Rightarrow \gamma > 0$$

Xi, Xu, Diamond, PRL 112, 085001 (2014)

γ_c is the critical growth rate and is determined by nonlinear interaction in the background turbulence

Summary (1)

As the pedestal collisionality decreases,
Two factors determine if a single mode amplitude can grow to a large magnitude to trigger an ELM

- ➢ **Linear growth rate**
- ➢ **Nonlinear growth time**

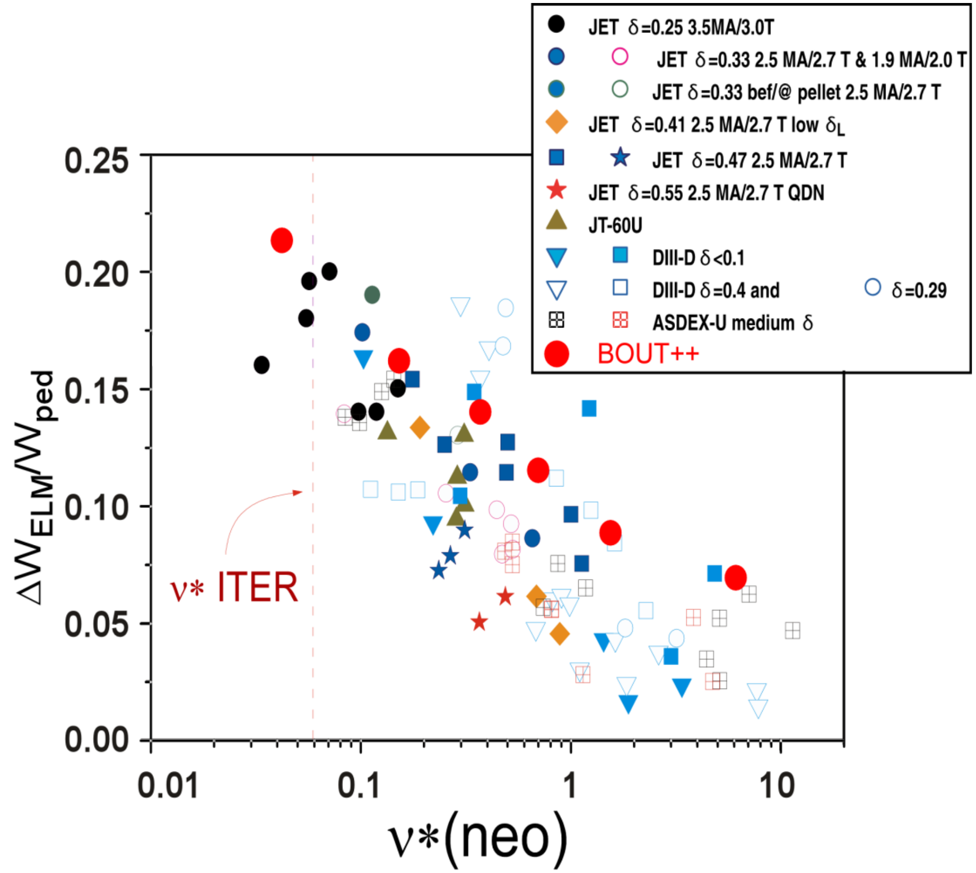

Part one: Linear results

The width of the growth rate spectrum γ(n) becomes narrower and the peak growth shifts to lower n

Part two: Nonlinear results

The growth time of linear drive is determined by nonlinear process via phase evolution for large ELM crash

Narrow mode spectrum → Weak nonlinear Phase Scattering →Long PCT →Large ELMs

BOUT++ simulations show consistent collisionality scaling of ELM energy losses with ITPA multi-tokamak database

Advanced Divertor Analysis of HL-2M

G.Y. Zheng[1], X.Q. Xu[2], D.D. Ryutov[2], T.Y. Xia[3] and Y.D. Pan[1], Z.H. Wang[1]

G.Y. Zheng

[1]Southwestern Institute of Physics, Chengdu, People's Republic of China
[2]Lawrence Livermore National Laboratory, Livermore, CA 94550, USA
[3]Institute of Plasma Physics, Chinese Academy of Sciences, Hefei, China

Presented at
the 25th IAEA Fusion Energy Conference (FEC 2014),
St Petersburg, Russian Federation
13 - 18 October 2014

HL-2M

HL-2M is a new tokamak under construction to study the high performance plasma, techniques and engineering issues relevant to fusion reactor.

Main plasma parameters

Plasma current	I_p = 2.5 (3) MA
Major radius	R = 1.78 m
Minor radius	a = 0.65 m
Aspect ratio	R/a = 2.8
Elongation	K = 1.8-2
Triangularity	δ > 0.5
Toroidal field	B_T = 2.2 (3) T
Flux swing	ΔΦ= 14Vs
Heating power	25 MW

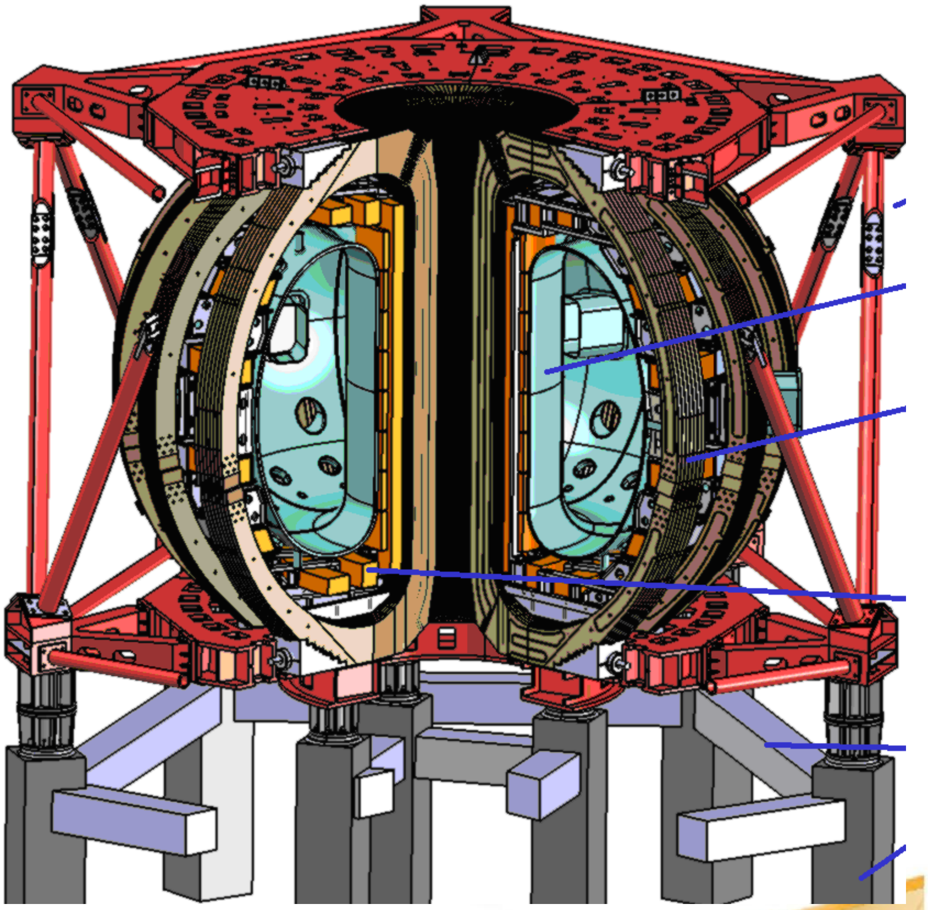

Main structure of HL-2M

HL-2M will be commissioned in 2015

The components of HL-2M are being fabricated.

Magnetic field coils

Vacuum vessel

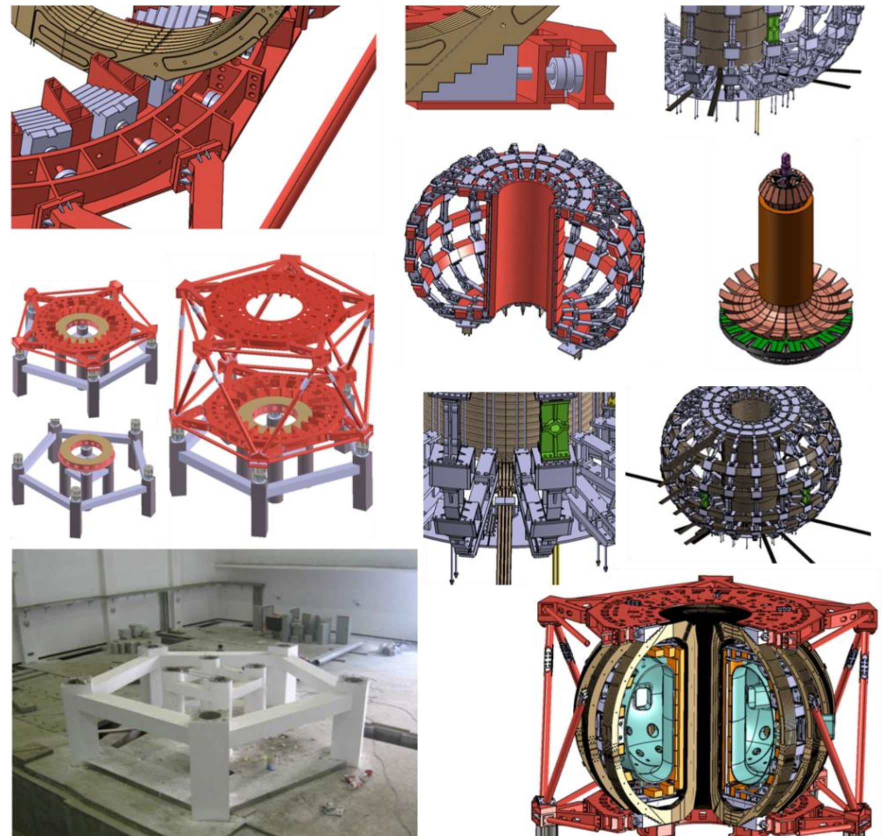

Support structure

High quality plasma and advanced divertor

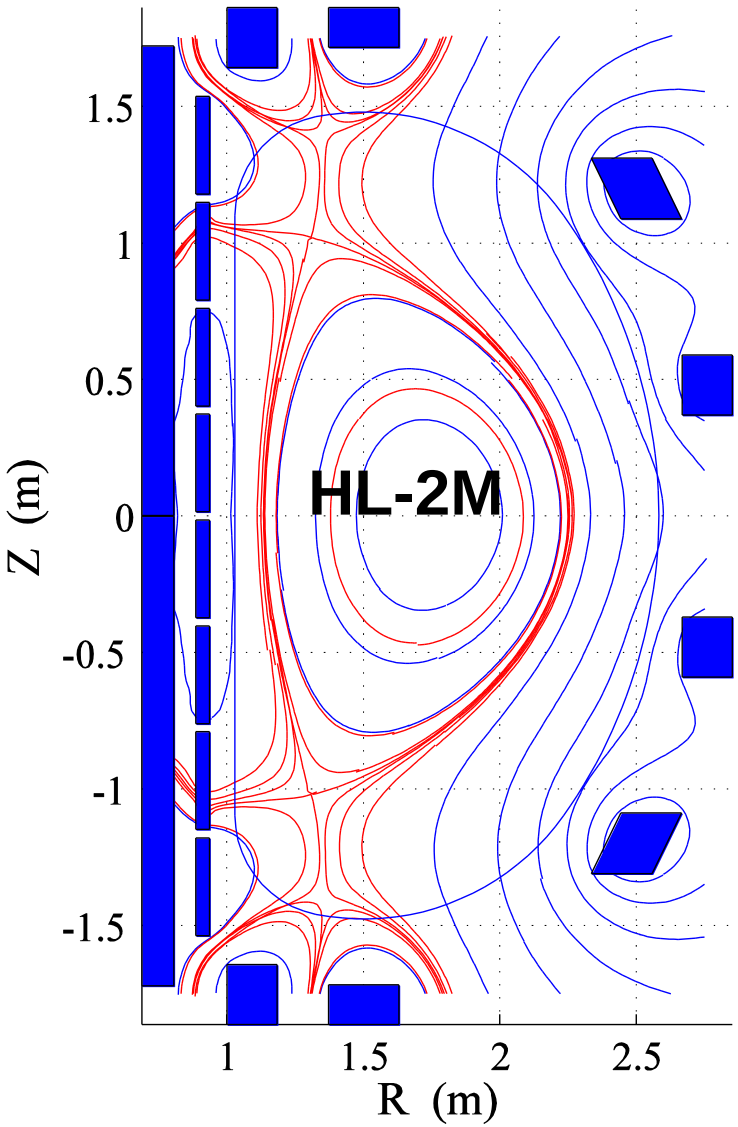

□HL-2M has a demountable TF coils with PF coils be placed inside the TF coils to enhance the flexibility and controllability of experiments to achieve high quality plasma;

Heat flux at target can be roughly compared

HL-2M: P/R = 14MW/m
ITER: P/R = 14~16MW/m

□PF coils close to core plasma, it will reduce the PF coils current to generate advanced divertor configuration with a second X point to handle large amount of heating power (25MW);

Advanced divertor configurations of HL-2M

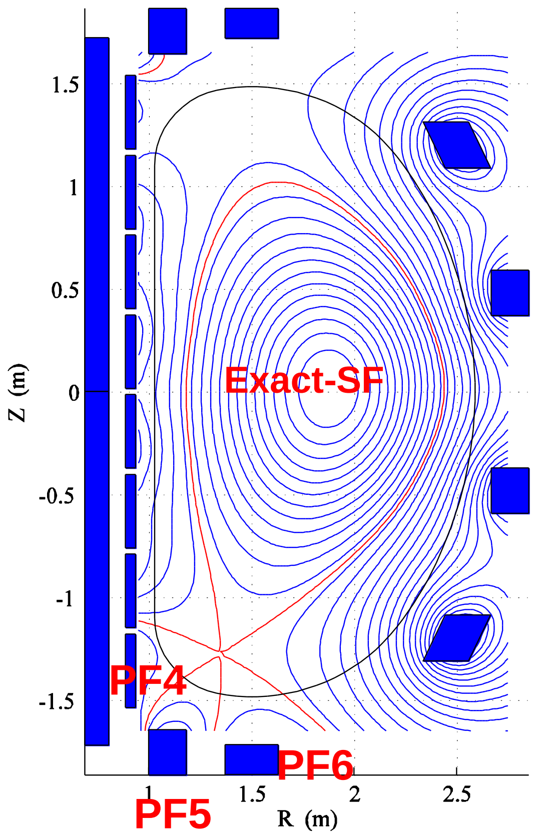

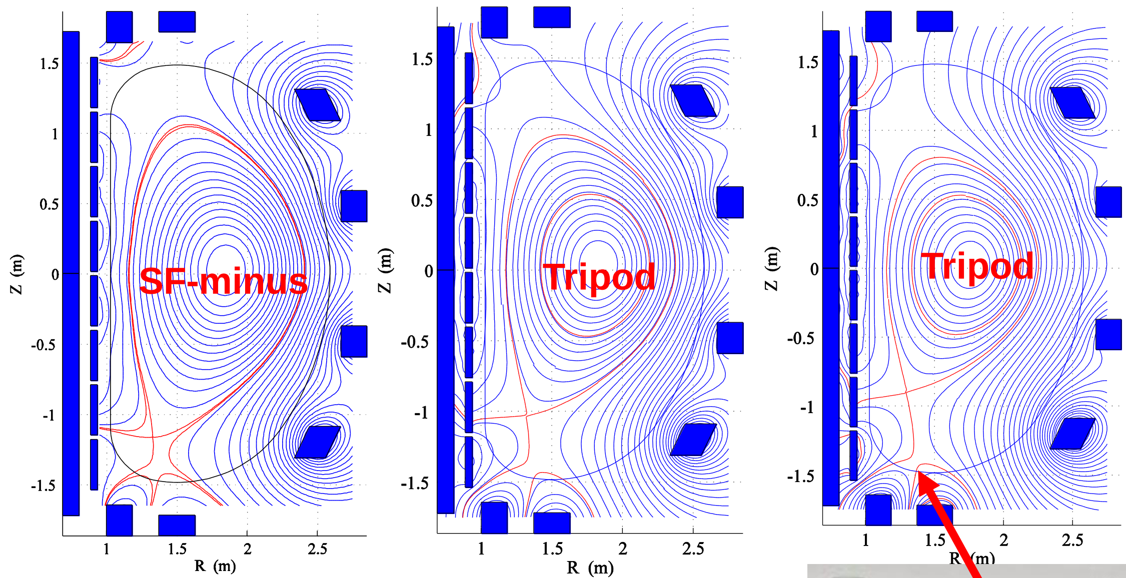

Configuration loses the features of a snowflake divertor, becomes just two separate X-points;

- A prototypical X-divertor or conceptually similar cusp divertor arranged coils near the strike point;
- we suggest to call a configuration with a long divertor leg and three outgoing branches of the separatrix a "tripod configuration".

Divertor target design of HL-2M

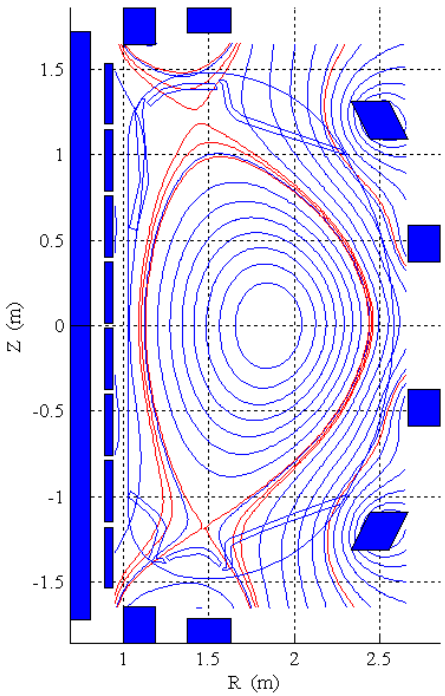

Standard divertor

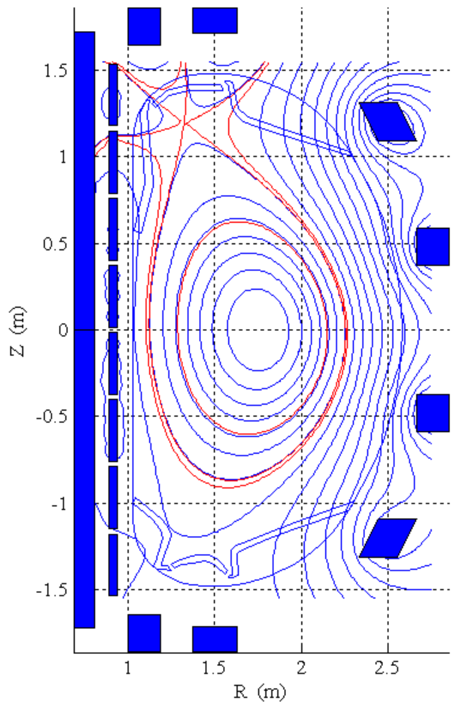

Exact-SF

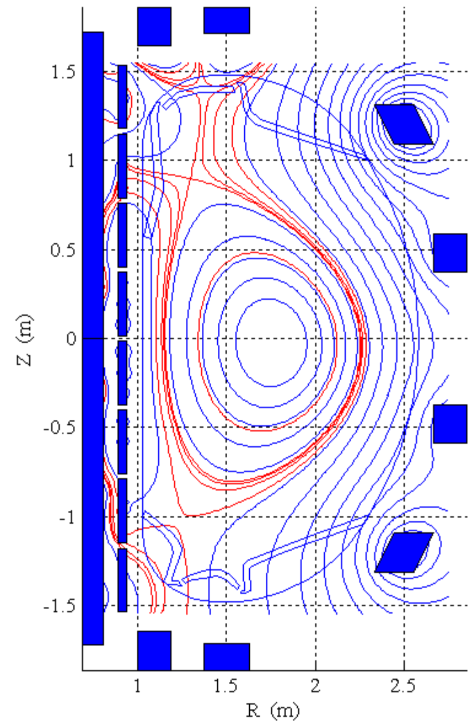

Tripod

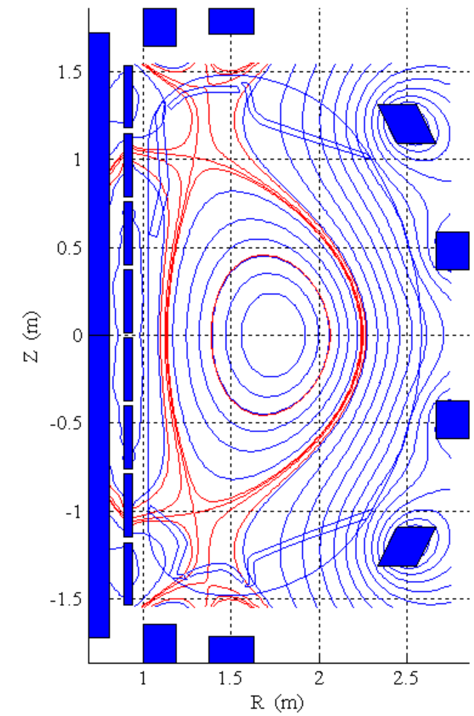

DN tripod

- Asymmetric divertor target
- Standard and advanced divertor
- Double Null divertor
- Target with large plasma-wetted area

Large Weak B_p area

SF-minus reduces P-B growth rate

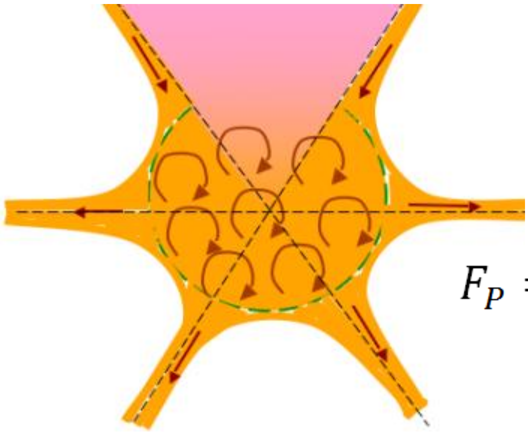

$$F_P = B_{p-point} / B_{p-mid}$$

$$\beta_{PM} \equiv 8\pi p / B_{PM}^2$$

D.D. Ryutov, et al., Contrib. Plasma Phys., 52, 539, 2012; PPCF, 54, 124050, 2012.

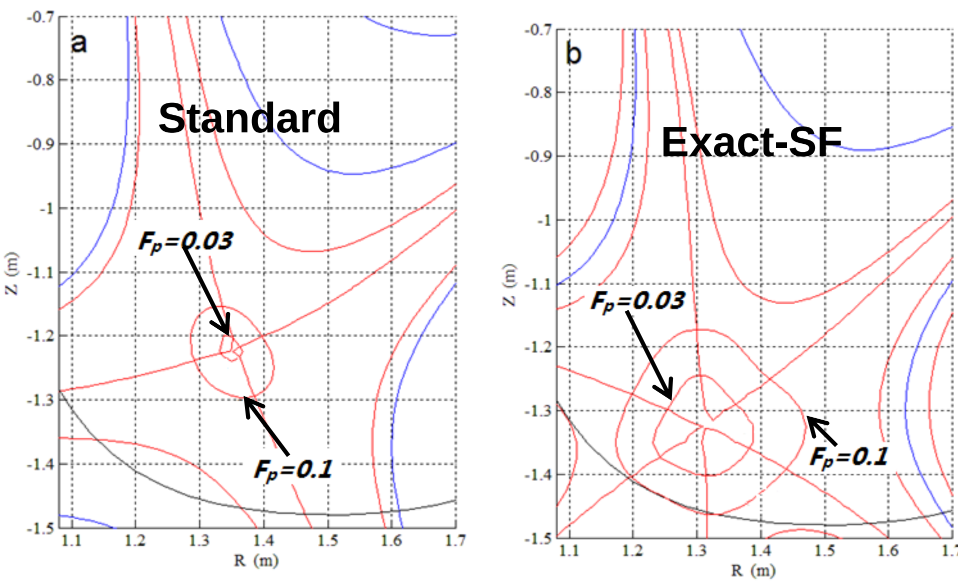

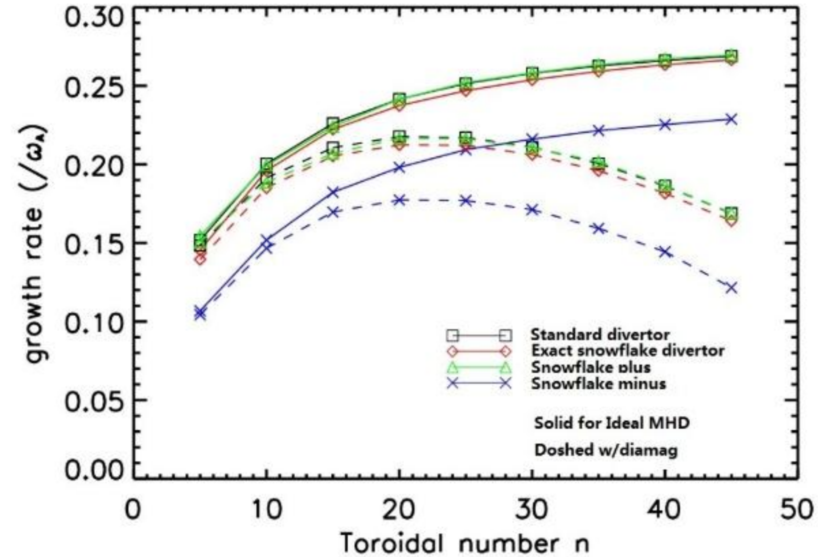

- Same main parameters, R, a, I_p, k_{95}, q_{95}.
- Same pressure and current profiles.

Fast convective heat transport around weak B_p can increase power sharing among the divertor legs and broaden the heat flux profile at target, especially during an ELM bursts

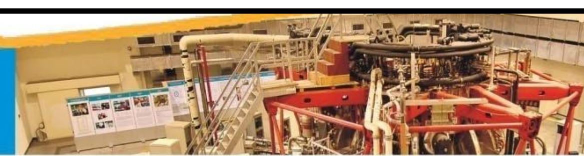

Heat flux at targets of DN tripod divertor

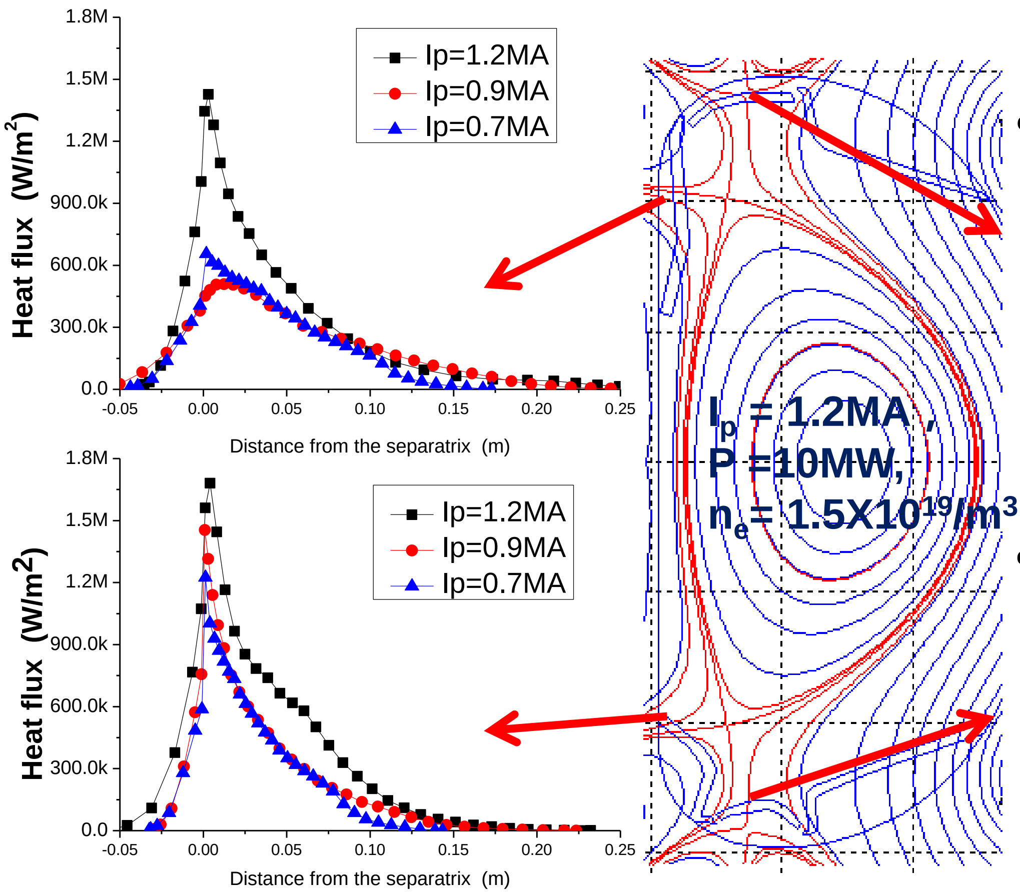

- Limit the power flows into inner divertor region;
- Handle most of heating power by outer divertor with longer connection length and large plasma-wetted area.

Summary (2)

- It is designed on HL-2M to achieve flexible divertor operation: standard, snowflake and tripod;

- Tripod divertor configuration is a new divertor configuration, in which the distance between two X points on divertor leg can be adjusted according to the plasma and PF coils parameters of HL-2M;

- HL-2M will have the ability to operate with high performance plasma and advanced divertor with 25MW heating power, and will be a platform to test the engineering and physics issues relevant to fusion reactor.

Thank you!

Summary

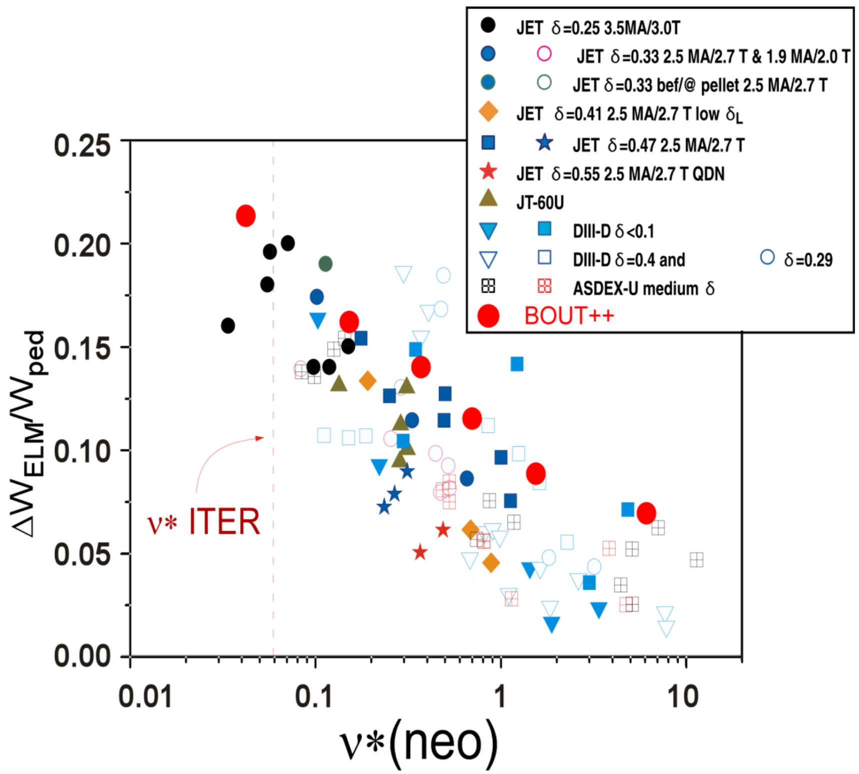

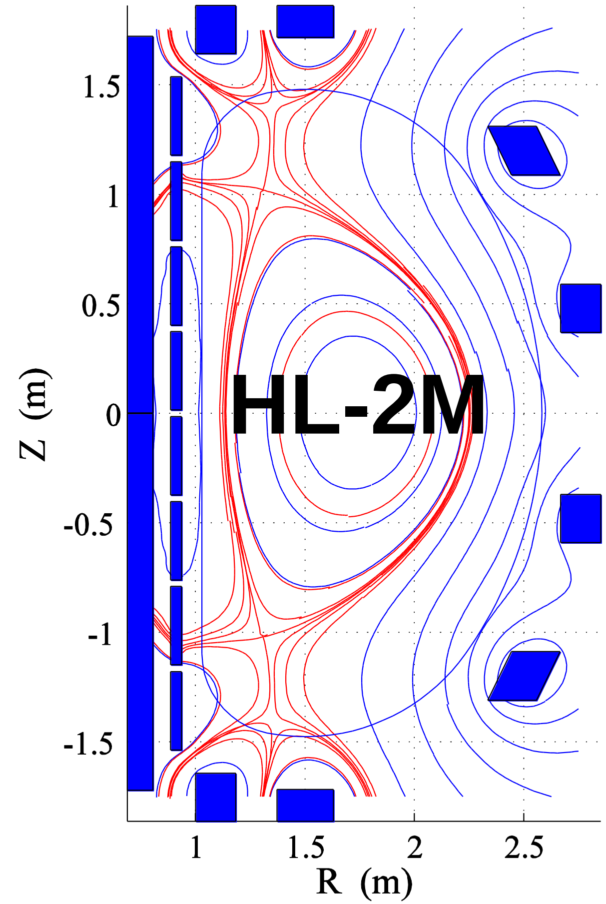

BOUT++ simulations show consistent collisionality scaling of ELM energy losses with ITPA multi-tokamak database

- ☐ **High performance plasma**
- ☐ **Advanced divertor**
- ☐ **25MW heating power**
- ☐ **Issues relevant to fusion reactor**

Simulation model and equilibrium in BOUT++

- **3-field model for nonlinear ELM simulations**
  - ✓ **Including essential physics for the onset of ELMs**

Peeling-ballooning instability
Resistivity
Hyper-resistivity
Ion diamagnetic effect

$$\frac{d\varpi}{dt} = B\nabla_\parallel J_\parallel + 2\mathbf{b}_0\times\boldsymbol{\kappa}\cdot\nabla\tilde{P} + \mu_{i,\parallel}\partial_\parallel^2\varpi$$

$$\frac{d\tilde{P}}{dt} + \mathbf{V}_E\cdot\nabla P_0 = 0$$

$$\frac{\partial A_\parallel}{\partial t} + \partial_\parallel\phi_T = \frac{\eta}{\mu_0}\nabla_\perp^2 A_\parallel - \frac{\eta_H}{\mu_0}\nabla_\perp^4 A_\parallel$$

$$\varpi = \frac{m_i n_0}{B}\left(\nabla_\perp^2\phi + \frac{1}{en_0}\nabla_\perp^2\tilde{P}_i\right)$$

$$d/dt = \partial/\partial t + \mathbf{V}_{ET}\cdot\nabla,\ \mathbf{V}_{ET} = \frac{1}{B}\mathbf{b}_0\times\nabla\phi_T,\ \phi_T = \phi_0 + \phi,\ \nabla_\parallel f = B\partial_\parallel\frac{f}{B},\ \partial_\parallel = \partial_\parallel^0 + \delta\mathbf{b}\cdot\nabla,\ \delta\mathbf{b} = \frac{1}{B}\nabla A_\parallel\times\mathbf{b}_0,\ J_\parallel = J_{\parallel 0} + \tilde{J}_\parallel,\ \tilde{J}_\parallel = -\nabla_\perp^2 A_\parallel/\mu_0$$

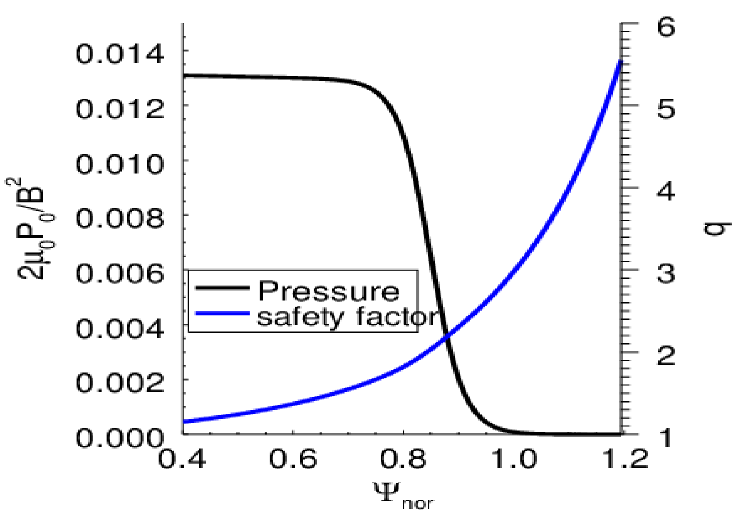

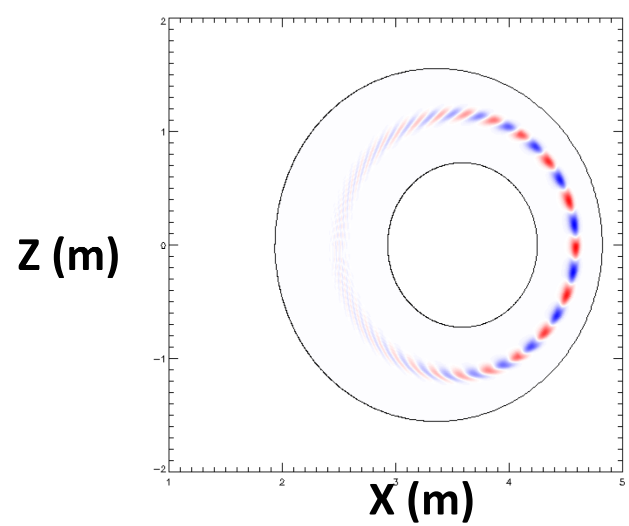

We create a set of equilibria with the self-consistent variation of density and temperature profiles, while keeping the plasma cross-sectional shape, total stored energy, total plasma current and pressure profile fixed.

- Eight cases: $n_e(0)$=1, 3, 5, 7, 9, 12, 15, 20x10^{19} m^{-3}.
- $n_e = n_e(0) * \left(\frac{P0}{P0(0)}\right)^{0.3}, T_e = \frac{P0}{2n_e}$.